LETTER

doi:10.1038/nature10321

A young source for the Hawaiian plume

Alexander V. Sobolev[1,2,3], Albrecht W. Hofmann[2,4], Klaus Peter Jochum[2], Dmitry V. Kuzmin[2,5] & Brigitte Stoll[2]

Recycling of oceanic crust through subduction, mantle upwelling, and remelting in mantle plumes is a widely accepted mechanism to explain ocean island volcanism[1]. The timescale of this recycling is important to our understanding of mantle circulation rates. Correlations of uranogenic lead isotopes in lavas from ocean islands such as Hawaii or Iceland, when interpreted as model isochrons, have yielded source differentiation ages between 1 and 2.5 billion years (Gyr)[2–5]. However, if such correlations are produced by mixing of unrelated mantle components[6] they will have no direct age significance. Re–Os decay model ages take into account the mixing of sources with different histories[7,8], but they depend on the assumed initial Re/Os ratio of the subducted crust, which is poorly constrained because of the high mobility of rhenium during subduction[9]. Here we report the first data on $^{87}Sr/^{86}Sr$ ratios for 138 melt inclusions in olivine phenocrysts from lavas of Mauna Loa shield volcano, Hawaii, indicating enormous mantle source heterogeneity. We show that highly radiogenic strontium in severely rubidium-depleted melt inclusions matches the isotopic composition of 200–650-Myr-old sea water. We infer that such sea water must have contaminated the Mauna Loa source rock, before subduction, imparting a unique 'time stamp' on this source. Small amounts of seawater-derived strontium in plume sources may be common but can be identified clearly only in ultra-depleted melts originating from generally highly (incompatible-element) depleted source components. The presence of 200–650-Myr-old oceanic crust in the source of Hawaiian lavas implies a timescale of general mantle circulation with an average rate of about 2 (±1) cm yr^{-1}, much faster than previously thought.

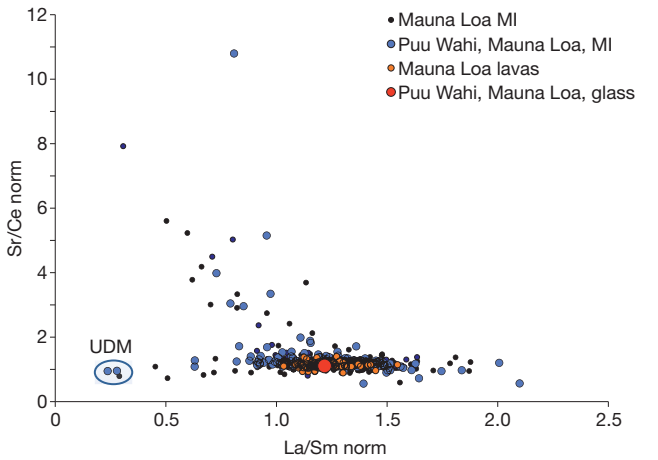

Figure 1 | Compositions of lavas and melt inclusions in olivine phenocrysts from recent (younger than 50 kyr) eruptions of Mauna Loa volcano, Hawaii. Data for Puu Wahi lava and melt inclusions (MI) are from this study; other melt inclusions are from ref. 13 and unpublished data of A.V.S. UDM inclusions are outlined. Compositions of Mauna Loa lavas are from the GEOROC database (http://georoc.mpch-mainz.gwdg.de/georoc/). All ratios are normalized to primitive mantle[31].

Melt inclusions in highly magnesian olivine are commonly used as proxies for parental melts[10]. In addition, melt inclusions provide unique information on the isotope heterogeneity of the mantle sources of ocean island basalts[11,12]. Compositions of melt inclusions in olivine (Supplementary Figs 1 and 2) from lavas of the largest Hawaiian shield volcano, Mauna Loa, vary considerably[13] (Fig. 1). Both La/Sm and Sr/Ce ratios of melt inclusions have very large (tenfold) variations, and this heterogeneity is much greater than those displayed by Mauna Loa bulk lava compositions. About 2–3% of melt inclusions are strongly depleted in the highly incompatible elements Th, U, Ba, Rb, K, Sr, Nb, Ta, Cl, B, Pb, S, Zr, Hf and the light rare-earth elements (Figs 1 and 2 and Supplementary Table 2). Here we will call these inclusions 'ultra-depleted melts' (UDMs). In contrast with typical Mauna Loa melts, UDMs are also slightly depleted in the moderately incompatible elements Ti, Nd, Sm and Al and are enriched in SiO_2, but are similar in contents of heavy rare-earth elements, Y, Sc and Ca (Fig. 2, Supplementary Fig. 3 and Supplementary Table 2). Strontium is significantly depleted relative to Pr, Nd and Sm. UDM inclusions have been reported in association with 'normal' inclusions in the same olivine grains[13]. In such an association, inclusions of mixed composition are commonly present. Mauna Loa UDMs have been interpreted[13] as instantaneous melts produced by near-fractional melting of Hawaiian source by a process that is similar to that described for mid-ocean-ridge UDM[14]. The isotope data presented here disprove this interpretation, showing that these UDMs also have significantly different source compositions from those of other parental melts.

Strontium and lead isotopic compositions of melt inclusions in olivine phenocrysts from a single Mauna Loa lava (see Supplementary Figs 1 and 2 for inclusion images) were measured by laser ablation inductively coupled plasma mass spectrometry (LA-ICP-MS; see

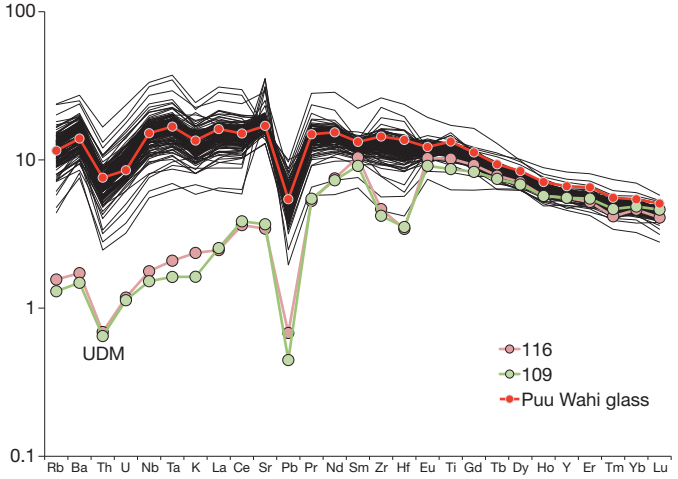

Figure 2 | Primitive mantle[31] normalized concentrations of incompatible elements in melt inclusions in euhedral olivine crystals from a single sample (K97-15b) of Puu Wahi scoria cone, Mauna Loa, Hawaii. Ultra-depleted melt inclusions are labelled UDM.

[1]ISTerre, University Joseph Fourier, Grenoble 1 and CNRS, BP 53, 38041 Grenoble, France. [2]Max Planck Institute for Chemistry, Postfach 3060, 55020 Mainz, Germany. [3]V. I. Vernadsky Institute of Geochemistry and Analytical Chemistry, Russian Academy of Sciences, Moscow 119991, Russia. [4]Lamont Doherty Earth Observatory, Palisades, New York 10964, USA. [5]V. S. Sobolev Institute of Geology and Mineralogy, Siberian Branch of Russian Academy of Sciences, Novosibirsk 630090, Russia.

Methods for sample description and analytical details). In total, 138 inclusions were analysed for Sr isotopes, and 106 inclusions for Pb isotopes. Both Sr and Pb isotopic compositions of melt inclusions vary markedly, much more than in Hawaiian lavas overall. But their averages are nevertheless similar in compositions to those of matrix glass and of typical recent Mauna Loa lavas (Fig. 3). The range of variation is markedly higher for melt inclusions trapped in the most magnesian olivines (Supplementary Fig. 4). This is consistent with the interpretation that melt inclusions in early-formed olivine phenocrysts yield information on the compositions of unmixed parental melts, whereas lavas and inclusions in more evolved olivines are mixtures of these melts[10,13]. Clear evidence of such mixing is presented by the most radiogenic melt inclusions with $^{87}Sr/^{86}Sr > 0.7060$. These inclusions consistently fit mixing trajectories for almost all incompatible elements and Sr isotopes, thus strengthening confidence in the reliability of the isotope data (Supplementary Fig. 5). UDMs represent the endmember of such mixing combining highly radiogenic Sr ($^{87}Sr/^{86}Sr = 0.7081 \pm 0.0006$, 2σ), much higher than the value of typical Mauna Loa melts ($^{87}Sr/^{86}Sr \approx 0.7038$), with Rb/Sr ratios (0.010–0.013) that are unusually low for Mauna Loa (Fig. 3a). Lead isotope compositions of UDMs are also significantly more radiogenic than those of typical Mauna Loa melts (Fig. 3b; note that the lowest $^{207}Pb/^{206}Pb$ ratios correspond to the most radiogenic Pb). These data clearly suggest that the UDMs could not have been produced from any typical Mauna Loa source by any melting process. Instead, the source rock must contain a component with highly radiogenic Sr and Pb, but must at the same time be strongly depleted in incompatible elements. Alternatively, this component might have been introduced by some type of contamination of the primary melt. Next we discuss possible sources.

Before presenting our preferred interpretation, namely source contamination by ancient sea water before subduction, we discuss alternative explanations. In general, the highly radiogenic Sr of Mauna Loa UDMs might be explained by one of the following processes, all of which have significant drawbacks.

First, direct input of recycled continental crust could in principle explain highly radiogenic Sr, but this is completely inconsistent with the extremely low concentrations of Rb, Ba, K, U and Pb, as well as their high Ce/Pb (50–80) and Nb/U (41–46) ratios[15].

Second, continental Sr might be transferred to the mantle source during subduction more indirectly by the percolation of crustal fluids without necessarily causing trace-element enrichment, if the mantle lithology is a depleted harzburgite containing no clinopyroxene. This process requires that, in addition to Sr, all other incompatible elements including Sc, Ca and Al in UDMs come from a clinopyroxene-free harzburgite source. However, this contradicts the relatively high contents of moderately incompatible elements (Ti, Al, Ca and rare-earth elements heavier than Sm) in UDMs that are similar to those of typical Mauna Loa melts (Fig. 2 and Supplementary Fig. 3), because harzburgites are typically depleted in all these elements. Additional observations that are very difficult to reconcile with any continental source, even in a markedly 'fractionated' form, are as follows: the very low Pb concentrations and high Ce/Pb ratios, as well as high Nb/U and Nb/Th ratios, are the opposite of what would be expected from a metasomatic (fluid) transfer of a sedimentary signature from a subducted slab or from recycled sediments (see Supplementary Information); and other ratios of trace elements of similar incompatibility (Ba, Rb, Th, U and Nb) are similar (though not identical) to those of oceanic basalts, in particular Hawaiian basalts, but quite different from those of continental materials.

Third, the radiogenic Sr might be derived directly or indirectly from modern sea water. Producing UDM by contamination with typical Mauna Loa melt is highly unlikely because such a contamination process cannot result in tenfold lower concentrations of most incompatible elements. Seawater assimilation would be somewhat more plausible if it affected the original, highly depleted melt (rather than normal Mauna Loa melt. Perhaps the most efficient mechanism for this would be the assimilation of recent aragonitic carbonate containing a high concentration of radiogenic Sr and depleted in all incompatible elements[16]. This process could add radiogenic Sr without significantly changing most of the incompatible-element budget of the melt. However, it would also increase Sr and Ca concentrations considerably. For example, a typical Mauna Loa melt with $^{87}Sr/^{86}Sr = 0.7040$ would require the assimilation of about 5% high-Sr carbonate to match the isotopic composition of UDM. This would result in a sixfold increase in Sr concentration of UDM if the carbonate contaminant contained 1,000 p.p.m. Sr, with $^{87}Sr/^{86}Sr = 0.7090$. This implies an unreasonably

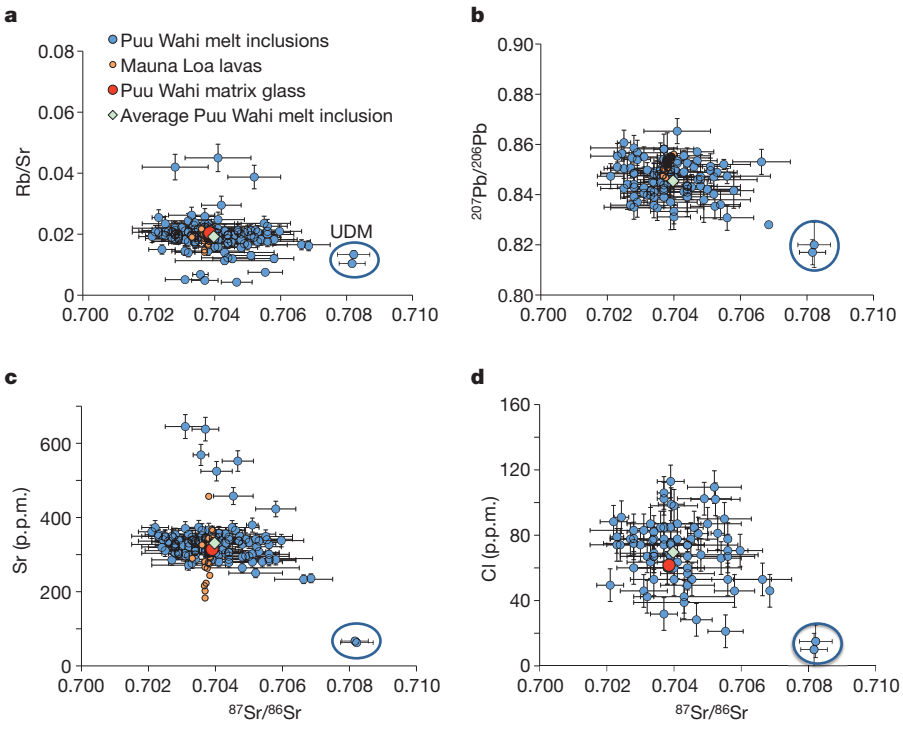

Figure 3 | $^{87}Sr/^{86}Sr$ ratios in melt inclusions and matrix glass in euhedral olivine crystals of sample (K97-15b), Puu Wahi scoria cone, Mauna Loa, Hawaii. a–d, $^{87}Sr/^{86}Sr$ ratios are plotted against Rb/Sr (**a**), $^{207}Pb/^{206}Pb$ (**b**), Sr (**c**) and Cl (**d**). Compositions of bulk Mauna Loa lavas from the GEOROC database are shown (in orange) for comparison. The compositions of average UDM inclusions are outlined. Error bars indicate s.e.m.

large negative Sr anomaly (half the primitive mantle value of Sr) in the initial, uncontaminated melt. Also, this process must increase the CaO content of the UDMs by at least 1.5 wt%, which is not observed (see Supplementary Fig. 3). Alternatively, seawater Sr might enter the melt by assimilation of highly altered ocean crust (including sediment). This could explain highly radiogenic Sr (Fig. 4) and low concentrations of incompatible elements, as well as more radiogenic Pb[17]. However, this should also incorporate other seawater-specific components, particularly B, Cl and K, because these elements are strongly enriched in altered crust[18]. But this is inconsistent with the extremely low concentrations of Cl (10–15 p.p.m.), B (0.3–0.4 p.p.m.) and K_2O (0.05–0.07 wt%) in the UDMs (Fig. 3d and Supplementary Table 2). Even if one assumes that these volatile elements were extracted from the assimilated crustal rocks by previous high-temperature metamorphism, this process still seems unlikely. To raise the originally low $^{87}Sr/^{86}Sr$ ratio of the melt to the highly radiogenic value observed, the amount of such assimilated material would have to be large. Such extensive assimilation would also affect concentrations of Ca, the heavy rare-earth elements, Y and Sc, all of which are relatively high and very similar in UDMs and typical Mauna Loa lavas (Fig. 2, Supplementary Fig. 3 and Supplementary Table 2). Alumina is slightly depleted in UDMs in comparison with Mauna Loa melts (Supplementary Fig. 3), and this also precludes the assimilation of any plagioclase-saturated, high-Al rocks, typical of oceanic crust. Similarly, we can rule out the assimilation of seawater-altered Hawaiian lavas, because of their high incompatible-element enrichment.

Reaction with altered harzburgites and their partial melting may also deliver highly radiogenic modern seawater Sr to depleted Mauna Loa

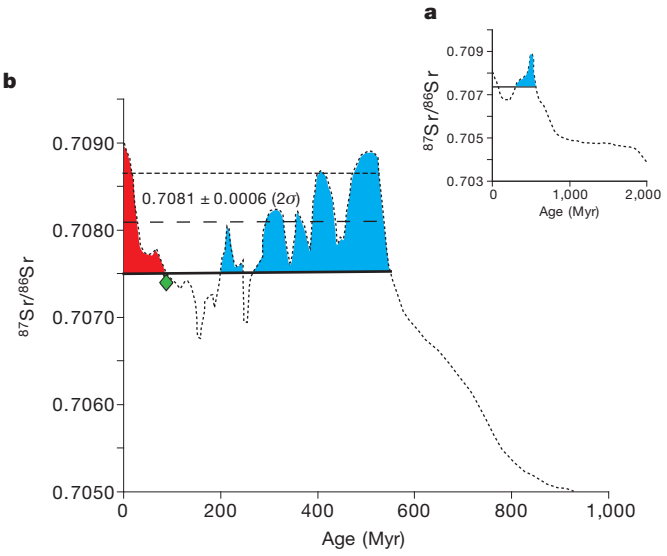

Figure 4 | $^{87}Sr/^{86}Sr$ ratios of the two most radiogenic Mauna Loa melt inclusions superimposed on the time evolution of Sr isotopic composition of sea water. **a**, Seawater evolution for the past 2 Gyr (ref. 22). **b**, Detailed Sr evolution for the past 1 Gyr (refs 19, 22). The green diamond indicates seawater composition at 90 Myr (ref. 19) corresponding to the age of lithosphere under the Big Island, Hawaii. The horizontal dashed line represents the pooled average $^{87}Sr/^{86}Sr$ ratio of 21 analyses of two UDM inclusions. The dotted line and heavy black line indicate the upper and lower limits of range of two standard errors of the average $^{87}Sr/^{86}Sr$, respectively. We suggest that the radiogenic Sr in UDMs is derived from ancient sea water in the Mauna Loa source (see the text). The blue field represents the acceptable age range for the recycled seawater component. We reject ages marked by the red field because we have ruled out recent seawater contamination (see the text). We consider the lower limit of the shown range ($^{87}Sr/^{86}Sr = 0.7075$, indicated on both panels) to be a minimum estimate for the composition of the seawater component in the Mauna Loa source, because its isotopic composition must have been diluted by less radiogenic components from the original unaltered basalt and source peridotite. The most likely age of recycled seawater Sr is in the range 200–550 Myr, but it may be extended to 650 Myr (ref. 23).

melt. But this process will also affect concentrations of Ni, Mn and Fe, which is not the case (Supplementary Fig. 8).

An additional argument against contamination by the present-day lithosphere beneath Hawaii is derived from the fact that this lithosphere is slightly more than 90 Myr old. At the time that it was created, sea water had a $^{87}Sr/^{86}Sr$ ratio of 0.7074 or less (ref. 19), just below the lower limit of UDM Sr (Fig. 4). Because seawater Sr is introduced into the altered crust almost entirely during the first 3 Myr after crust formation[20], it is highly unlikely that Sr contamination derived from 90-Myr-old lithosphere can account for the observed composition ($^{87}Sr/^{86}Sr \geq 0.7075$) of the UDMs.

Because none of the above processes provides a satisfactory explanation for the presence of highly radiogenic Sr and Pb in the UDM, we suggest that the radiogenic Sr was introduced through direct or indirect contamination by ancient sea water before subduction and recycling. In this case, other indicators of sea water or seawater alteration, K, B and Cl, should easily be removed from the system by mobilization during subduction[21]. In addition, Ca, Al, rare-earth elements, Sc and Y in the melt would be constrained by the mineralogy of the mantle residue, specifically by the presence of garnet and high-Ca pyroxene. However, Sr in ancient sea water was, during most of Earth's history, much less radiogenic than Sr in the UDMs, except for one specific time window, namely the period between 200 and 550 Myr ago[19,22] (Fig. 4). According to other estimates[23] this period may be extended at maximum to 650 Myr. Therefore, if the effect is indeed caused by recycled seawater Sr, this sea water is unlikely to be older than 650 Myr old.

We propose that Mauna Loa UDMs reveal one of the recycled end-member compositions similar to ultra-depleted mid-ocean-ridge basalt (MORB)[14] or gabbros[24] with Sr extensively exchanged with, and dominated by, seawater Sr because of its initially low content (see model in Methods). This explanation is also consistent with the strong negative Zr anomaly in Mauna Loa UDMs, which is a common feature of ultra-depleted MORB as well[14]. Highly depleted gabbronorites crystallized from remelted material of this kind possessing $^{87}Sr/^{86}Sr$ up to ~0.708 have been reported in oceanic crust exposed in the Oman ophiolite[25]. The Sr isotopes of the other recycled rocks (typical gabbros or normal MORBs) indicated by the compositions of melt inclusions (Fig. 3) were less affected by seawater alteration because of their higher Sr contents and/or different positions in the crust[18]. The Sr-rich component of Mauna Loa lavas is particularly unradiogenic ($^{87}Sr/^{86}Sr < 0.7030$; see Fig. 3c), in agreement with its origin from recycled oceanic plagioclase-cumulate gabbros[13]. Alternatively, seawater Sr might be introduced into the subduction 'package' by means of serpentinites or carbonate veins that are ubiquitous in the oceanic crust. Particularly when precipitated at low temperatures, they preserve the Sr isotopic composition of sea water[16]. We further suggest that all these recycled materials have been processed during subduction to remove most of the additional Cl, B, Rb and K introduced by sea water.

Previous estimates of recycling times in mantle plumes have mostly relied on Pb isotopes. If an initially homogeneous source is differentiated (for example, by melting) into subsystems with variable U/Pb ratios, these subsystems evolve to a linear isochron in $^{207}Pb/^{204}Pb$–$^{206}Pb/^{204}Pb$ space. Such linearly correlated Pb isotopes are widespread in oceanic basalts and have frequently been interpreted as isochrons corresponding to recycling ages ranging from 1.0 to 2.5 Gyr (ref. 2). However, they might also simply represent mixing lines between unrelated reservoirs[6]. It has been pointed out[26] that the isochron interpretation fails when Th/U ratios inferred from the slope of $^{208}Pb/^{204}Pb$–$^{206}Pb/^{204}Pb$ correlations are inconsistent with observed Th/U ratios in the rocks, and it was concluded that the Pb isotope correlations for Mauna Kea must represent mixing lines rather than isochrons.

All Mauna Loa olivine phenocrysts possess Ni excess and Mn deficiencies, which suggests the involvement of melts from olivine-free reaction pyroxenite and peridotite sources in proportions of about

60:40, respectively[27,28] (Supplementary information). From one-half to two-thirds of this reaction pyroxenite is derived from high-silica melt from recycled crust in the form of eclogite, with the other part being peridotite[27]. In total this yields 60–70% peridotite component in the source of Mauna Loa magma. However, because $^{87}Sr/^{86}Sr$ in the UDMs is nearly at the maximum possible value for sea water[19], this implies that most of the Sr, as well as other incompatible elements, came from the recycled crustal component. This leaves very little room for peridotite-derived incompatible elements, and thus requires that the peridotitic component was severely depleted in these elements, including Sr, so that it did not significantly affect the incompatible element budget of the final melt (see Methods and Supplementary Information for the quantitative model). Alternatively, peridotite could be moderately depleted in incompatible elements, but it would contain radiogenic Sr resulting from seawater alteration, and this would represent part of the recycled oceanic lithosphere.

Our interpretation of the UDM compositions implies an age for the recycled component in the Mauna Loa source of between 200–650 Myr, much younger than previously suggested source differentiation ages of deep mantle plumes[2–5,7,8]. Such a young age is consistent with a timescale of general mantle circulation with an average rate of about 1–3 cm yr^{-1}, assuming that subducted crust was delivered to the core–mantle boundary at 2,900 km depth, and the Hawaiian plume rises from that depth.

METHODS SUMMARY

The picritic sample K97-15b from Puu Wahi scoria cone (age 910 yr), Mauna Loa volcano, Hawaii, contains euhedral olivine grains (Fo 89–82) with naturally quenched melt inclusions and matrix glass.

Major and some trace elements in melt inclusions, glass and host olivines were determined by electron probe microanalysis on a Jeol JXA 8200 SuperProbe Electron Probe Microanalyser at the Max Planck Institute for Chemistry (MPIC) Mainz, Germany, with a 2σ relative error of 1–2%. The compositions of olivine and contents of Cl, S, Ni and Cr in inclusions were analysed by following a special procedure that allows precision and accuracy of 20–30 $\mu g\,g^{-1}$ (2σ error) for Ni, Ca, Mn, Al, Ti, Cr and Co, 0.02 mol% for the forsterite component in olivine[28], 4 $\mu g\,g^{-1}$ for Cl and 20 $\mu g\,g^{-1}$ for S in glass.

LA-ICP-MS was used to determine trace elements in glasses of melt inclusions on an Element-2, Thermo Scientific mass spectrometer with a UP-213 New Wave Research solid-phase laser at MPIC, with a precision and accuracy of about 10–15% (2 relative standard deviations (r.s.d.)). Boron concentrations were measured by secondary-ion mass spectrometry on a Cameca Ims-3f ion probe at MPIC with an accuracy and precision of about 20% (2 r.s.d.).

In situ Sr and Pb isotope analyses of melt inclusions were performed at MPIC with the ICP mass spectrometer Thermo Element-2 and the New Wave UP 193 laser ablation system with a precision and accuracy of about 0.02–0.10% (1 r.s.d.) for Sr (new data and ref. 29) and 0.1% $^{208}Pb/^{206}Pb$ and $^{207}Pb/^{206}Pb$ (ref. 30) for one-to-three-spot analyses of melt inclusions.

Quantitative modelling suggests that highly radiogenic Sr and the chemical composition of Mauna Loa UDMs can result from recycling, melting and reacting of depleted oceanic crust altered by sea water and depleted mantle peridotite.

Full Methods and any associated references are available in the online version of the paper at www.nature.com/nature.

Received 31 July 2010; accepted 17 June 2011.
Published online 10 August 2011.

1. Hofmann, A. W. & White, W. M. Mantle plumes from ancient oceanic crust. *Earth Planet. Sci. Lett.* **57,** 421–436 (1982).
2. Chase, C. G. Oceanic island Pb: two-stage histories and mantle evolution. *Earth Planet. Sci. Lett.* **52,** 277–284 (1981).
3. McKenzie, D. *et al.* Source enrichment processes responsible for isotopic anomalies in oceanic island basalts. *Geochim. Cosmochim. Acta* **68,** 2699–2724 (2004).
4. Sun, S. S. & Hanson, G. N. Origin of Ross Island basanitoids and limitations upon the heterogeneity of mantle sources for alkali basalts and nephelinites. *Contrib. Mineral. Petrol.* **52,** 77–106 (1975).
5. Tatsumoto, M. Isotopic composition of lead in oceanic basalt and its implication to mantle evolution. *Earth Planet. Sci. Lett.* **38,** 63–87 (1978).
6. Farnetani, C. G. & Hofmann, A. W. Dynamics and internal structure of a lower mantle plume conduit. *Earth Planet. Sci. Lett.* **282,** 314–322 (2009).
7. Brandon, A. D., Graham, D. W., Waight, T. & Gautason, B. ^{186}Os and ^{187}Os enrichments and high-$^{3}He/^{4}He$ sources in the Earth's mantle: evidence from Icelandic picrites. *Geochim. Cosmochim. Acta* **71,** 4570–4591 (2007).
8. Sobolev, A. V., Hofmann, A. W., Brügmann, G., Batanova, V. G. & Kuzmin, D. V. A quantitative link between recycling and osmium isotopes. *Science* **321,** 536 (2008).
9. Sun, W. D., Bennett, V. C. & Kamenetsky, V. S. The mechanism of Re enrichment in arc magmas: evidence from Lau Basin basaltic glasses and primitive melt inclusions. *Earth Planet. Sci. Lett.* **222,** 101–114 (2004).
10. Sobolev, A. V. Melt inclusions in minerals as a source of principal petrological information. *Petrology* **4,** 209–220 (1996).
11. Saal, A. E., Hart, S. R., Shimizu, N., Hauri, E. H. & Layne, G. D. Pb isotopic variability in melt inclusions from oceanic island basalts, Polynesia. *Science* **282,** 1481–1484 (1998).
12. Jackson, M. G. & Hart, S. R. Strontium isotopes in melt inclusions from Samoan basalts: implications for heterogeneity in the Samoan plume. *Earth Planet. Sci. Lett.* **245,** 260–277 (2006).
13. Sobolev, A. V., Hofmann, A. W. & Nikogosian, I. K. Recycled oceanic crust observed in 'ghost plagioclase' within the source of Mauna Loa lavas. *Nature* **404,** 986–990 (2000).
14. Sobolev, A. V. & Shimizu, N. Ultra-depleted primary melt included in an olivine from the Mid-Atlantic Ridge. *Nature* **363,** 151–154 (1993).
15. Hofmann, A. W. in *Treatise on Geochemistry* Vol. 2 (eds Holland, H. D. & Turekian, K. K.) 61–101 (Elsevier, 2003).
16. Coggon, R. M., Teagle, D. A. H., Smith-Duque, C. E., Alt, J. C. & Cooper, M. J. Reconstructing past seawater Mg/Ca and Sr/Ca from mid-ocean ridge flank calcium carbonate veins. *Science* **327,** 1114–1117 (2010).
17. Muinos, S. B. *et al.* New constraints on the Pb and Nd isotopic evolution of NE Atlantic water masses. *Geochem. Geophys. Geosyst.* **9,** Q02007 (2008).
18. Staudigel, H., Plank, T., White, W. M. & Schmincke, H. U. in *SUBCON: Subduction from Top to Bottom* Vol. 96 (eds Bebout, G. E. & Kirby, S. H.) 19–38 (American Geophysical Union, 1996).
19. Veizer, J. *et al.* Sr-87/Sr-86, delta C-13 and delta O-18 evolution of Phanerozoic seawater. *Chem. Geol.* **161,** 59–88 (1999).
20. Staudigel, H., Hart, S. R. & Richardson, S. H. Alteration of the oceanic crust: Processes and timing. *Earth Planet. Sci. Lett.* **52,** 311–327 (1981).
21. Marschall, H. R., Altherr, R. & Rupke, L. Squeezing out the slab—modelling the release of Li, Be and B during progressive high-pressure metamorphism. *Chem. Geol.* **239,** 323–335 (2007).
22. Shields, G. & Veizer, J. Precambrian marine carbonate isotope database: version 1.1. *Geochem. Geophys. Geosyst.* **3,** 1031 (2002).
23. Halverson, G. P., Dudas, F. O., Maloof, A. C. & Bowring, S. A. Evolution of the $^{87}Sr/^{86}Sr$ composition of Neoproterozoic seawater. *Palaeogeogr. Palaeoclimatol. Palaeoecol.* **256,** 103–129 (2007).
24. Ross, K. & Elthon, D. Cumulates from strongly depleted mid-ocean-ridge basalt. *Nature* **365,** 826–829 (1993).
25. Benoit, M., Ceuleneer, G. & Polvé, M. The remelting of hydrothermally altered peridotite at mid-ocean ridges by intruding mantle diapirs. *Nature* **402,** 514–518 (1999).
26. Abouchami, W., Galer, S. J. G. & Hofmann, A. W. High precision lead isotope systematics of lavas from the Hawaiian Scientific Drilling Project. *Chem. Geol.* **169,** 187–209 (2000).
27. Sobolev, A. V., Hofmann, A. W., Sobolev, S. V. & Nikogosian, I. K. An olivine-free mantle source of Hawaiian shield basalts. *Nature* **434,** 590–597 (2005).
28. Sobolev, A. V. *et al.* The amount of recycled crust in sources of mantle-derived melts. *Science* **316,** 412–417 (2007).
29. Jochum, K. P., Stoll, B., Weis, U., Kuzmin, D. V. & Sobolev, A. V. *In situ* Sr isotopic analysis of low Sr silicates using LA-ICP-MS. *J. Anal. At. Spectrom.* **24,** 1237–1243 (2009).
30. Jochum, K. P., Stoll, B., Herwig, K. & Willbold, M. Improvement of *in situ* Pb isotope analysis by LA-ICP-MS using a 193 nm Nd:YAG laser. *J. Anal. At. Spectrom.* **21,** 666–675 (2006).
31. McDonough, W. F. & Sun, S. S. The composition of the Earth. *Chem. Geol.* **120,** 223–253 (1995).

Supplementary Information is linked to the online version of the paper at www.nature.com/nature.

Acknowledgements We thank A. T. Anderson for providing the Puu-Wahi sample, N. Groschopf for help in managing the electron probe microanalyser, A. Yasevich and O. Kuzmina for sample preparation, and G. Wörner, N. Arndt and F. Holtz for discussions. This study was funded by an Agence Nationale de la Recherche, France, Chair of Excellence grant (ANR-09-CEXC-003-01) to A.V.S.. Partial support by a Gauss Professorship in Göttingen University, Germany, the Russian Foundation for Basic Research (09-05-01193a), a Russian President grant for leading Russian scientific schools (НШ-3919.2010.5), and Earth Sciences Department of Russian Academy grants to A.V.S. are also acknowledged. This is Lamont Doherty Earth Observatory contribution 7479.

Author Contributions A.V.S. designed the project. A.V.S. and A.W.H. conceived the interpretation and the model and wrote the paper. K.P.J. developed the analytical methods for isotope measurements by LA-ICP-MS. D.V.K. processed samples. D.V.K. and B.S. took the measurements. All authors contributed intellectually to the paper.

Author Information Reprints and permissions information is available at www.nature.com/reprints. The authors declare no competing financial interests. Readers are welcome to comment on the online version of this article at www.nature.com/nature. Correspondence and requests for materials should be addressed to A.V.S. (alexander.sobolev@ujf-grenoble.fr).

METHODS

Samples. The sample K97-15b has been collected by Alfred Anderson at Puu Wahi, from a scoria cone of 910-year-old picritic lava situated at about 3,000 m elevation on the northeast rift zone of Mauna Loa volcano, Hawaii. The melt inclusions hosted by euhedral olivine grains (Fo 89–82) of millimetre size were naturally quenched during eruption and formed fresh glass and small (a few volume per cent) low-density shrinkage bubbles (Supplementary Fig. 1).

Isotope analyses. *In situ* Sr and Pb isotope analyses of melt inclusions were performed at the Max Planck Institute for Chemistry in 2006, with the ICP mass spectrometer Thermo Element-2 and the New Wave UP 193 laser ablation system (wavelength 193 nm, energy density 4 J cm^{-2}, spot sizes 50 μm (Sr) and 75–100 μm (Pb), pulse repetition rate 10 Hz)[29,30]. In addition, Sr was remeasured in October 2010 and February 2011 after improvements of the detection system, to reaffirm and improve the overall reliability of the Sr isotope results.

The precision and accuracy of our LA-ICP-MS method in measuring $^{87}Sr/^{86}Sr$ ratios was constrained by analysing well-documented reference glasses (see Supplementary Table 1). The external precision of data obtained in 2006 was reported in ref. 29 as the standard deviation (s.d.) of sample measurements and is a strong function of Sr content of glasses (see Supplementary Fig. 6). From this equation (obtained for the reference glasses) one can predict s.d. = 0.0010 for UDMs containing 65 p.p.m. Sr. For the nine individual UDM measurements in 2006 the corresponding predicted standard error of the mean (s.e.m.) is 0.0003. These predicted values are slightly smaller than the actually observed s.d. of 0.0016 and 0.0005 for UDMs. This result is to be expected because reference glasses are significantly larger in all three dimensions than the measured inclusions and generally yield a somewhat larger number of total counts, yielding slightly higher precision.

To substantiate our results and further improve precision we reanalysed (in October 2010) the Sr isotope ratios of 21 melt inclusions, including both UDMs, using a significantly upgraded LA-ICP-MS system providing a combined effect of an improved stability and higher sensitivity. The improvements include a new multiplier system, a new ion detection unit and front-end computer of the ICP mass spectrometer, and new adjustment of the laser including cleaning of the valves and tubing in the laser ablation system. These technical improvements led to a laser fluence that was higher (about 10 J cm^{-2} in comparison with about 4 J cm^{-2}) and more uniform (decrease to about 2% during 4 h of operation, from about 25% before the improvements), higher counting rates (by about twofold) and lower blanks (for example, for ^{88}Sr about 70 c.p.s. in comparison with 300 c.p.s.[29]).

The higher precision and accuracy of the new data, for low-Sr samples, is clearly shown by new analyses of the reference glasses (Supplementary Fig. 6 and Supplementary Table 1), performed concurrently with those of the inclusions. Note that all natural reference glasses yield means of measured $^{87}Sr/^{86}Sr$ ratios within one standard error of the reference value, which proves that the standard error is an appropriate measure of both precision and accuracy. The predicted maximum precision (and accuracy) of $^{87}Sr/^{86}Sr$ ratios for the new measurements of UDM inclusions, estimated from these data, is s.d. = 0.0004 for an individual measurement and s.e.m. = 0.0001 for the mean of 12 measurements. A significant advance in precision of UDMs and reference glasses with similar low Sr contents is evident from Supplementary Tables 1 and 3. All reanalysed melt inclusions match the older data set very well but with better precision (see Supplementary Fig. 7). The new data for 12 individual measurements of the UDM yield $^{87}Sr/^{86}Sr = 0.7082 \pm 0.0006$ (two s.e.m.). If we pool the old and the new data, we have 21 measurements yielding a virtually identical mean value of $^{87}Sr/^{86}Sr = 0.7081 \pm 0.0006$ (two s.e.m.). Although the precision of the new data are somewhat better than that of the older analyses, we use the full data set of 21 analyses because the two data sets, separated by a time gap of four years, show excellent consistency.

Analysis of major and trace elements. Major and trace elements were determined by electron probe microanalysis on a Jeol JXA 8200 SuperProbe Electron Probe Microanalyser at MPIC, Mainz, Germany. Major-element abundances in glasses were measured at an accelerating voltage of 15 kV and a beam current of 12 nA with a reference sample of natural basaltic glass USNM111240/52 (VG2)[32] with a relative error of 1–2%. The compositions of olivines and Cl, S, Ni and Cr in glasses were analysed at an accelerating voltage of 20 kV and a beam current of 300 nA, by following a special protocol[28] that allowed 20–30 p.p.m. (2σ error) precision and accuracy for Ni, Ca, Mn, Al, Ti, Cr and Co, and 0.02 mol% for the forsterite component in olivine and 20 p.p.m. for Cl and S in glass.

Trace elements in glasses of melt inclusions were determined by LA-ICP-MS on an Element-2, Thermo Scientific mass spectrometer with a UP-213 New Wave Research solid-phase laser at MPIC, with reference to the KL-2G and NIST 612 standard glasses[33] (see http://georem.mpch-mainz.gwdg.de). Ca was used as a reference element. The typical conditions were: laser diameter 60–80 μm, energy density about 7 J cm^{-2}, pulse repetition rate 10 Hz and ablation time 60–80 s. The element abundances were determined with 2σ errors of no more than 5% and 10% for concentrations above 1 p.p.m. and ~0.1 p.p.m., respectively.

Boron content in glasses of melt inclusions was measured by secondary-ion mass spectrometry on a Cameca Ims3F ion microanalyser at MPIC with reference to the KL-2G and NIST 612 standard glasses by following the protocol[10] with a relative error commonly within 10%. The detection limit for B, estimated from ^{11}B intensity on the host olivine, was below 0.02 p.p.m.

Modelling. According to our model, the parental Hawaiian melts are mixtures of melts produced by the melting of olivine-free reaction pyroxenite and peridotite in which the proportion of pyroxenite-derived melt (X_{PX}) is estimated from the olivine composition[27,28]. The pyroxenitic source is generated by reaction between high-Si, eclogite-derived melt and peridotite, with the proportion of reactive melt (φ) similar to the original amount of olivine in peridotite[27]. The other variables that constrain the composition of the final melt are: degrees of melting of eclogite (F_E) and peridotite (F_{PE}), their chemical, isotopic and phase compositions, the degree of melting of pyroxenite (F_{PX}), melting reactions, and partition coefficients between melt and crystals. Mass conservation requires the following relations between the contents of bulk Sr, ^{86}Sr and ^{87}Sr in the final mantle-derived, primary melt (PM), peridotite (PE) and eclogite (E) for a batch melting process:

$$i_{Sr_{PM}} = i_{Sr_{PE}} \times \left[\frac{X_{PX}\times(1-\varphi)}{F_{PX}+(1-F_{PX})\times K_{PX}^{Sr}} + \frac{(1-X_{PX})}{F_{PE}+(1-F_{PE})\times K_{PE}^{Sr}}\right] + i_{Sr_E} \times \frac{\varphi \times X_{PX}}{(F_{PX}+(1-F_{PX})\times K_{PX}^{Sr})\times(F_E+(1-F_E)\times K_E^{Sr})} \quad (1)$$

where $i = 86$ or 87, nd (bulk Sr) K_{PX}^{Sr}, K_{PE}^{Sr} and K_E^{Sr} are bulk distribution coefficients for Sr or its isotopes between crystal phases and melt for pyroxenite, peridotite and eclogite, respectively.

$$^{86}Sr_j = \frac{Sr_j}{^{87}Sr_j/^{86}Sr_j + (^{84}Sr_j + ^{86}Sr_j + ^{88}Sr_j)/^{86}Sr_j} \quad (2)$$

where j = PM, PE or E, and the ratio of unradiogenic stable isotopes $(^{84}Sr_j + ^{86}Sr_j + ^{88}Sr_j)/^{86}Sr_j = 9.43205$.

Equation (1) for Sr, ^{87}Sr and ^{86}Sr and equation (2) for primary melt, eclogite and peridotite give six equations with nine unknowns (Sr_{PE}, $^{87}Sr_{PE}$, $^{86}Sr_{PE}$, Sr_{PM}, $^{87}Sr_{PM}$, $^{86}Sr_{PM}$, Sr_E, $^{87}Sr_E$ and $^{86}Sr_E$). To resolve these equations one needs to constrain three unknowns. The seawater model presented in this paper allows a maximum $^{87}Sr/^{86}Sr$ ratio of recycled eclogite of 0.7090 (first constraint), while the measured composition of the UDMs requires the minimum $^{87}Sr/^{86}Sr$ ratio of the final melt to be 0.7075 (second constraint; see Fig. 4). The composition of the UDMs also allows the composition of primary UDM to be estimated by reversing olivine fractionation up to equilibrium with the most magnesian olivine for Mauna Loa (Fo 90.7; ref. 27). This yields Sr_{PM} = 51 p.p.m. Sr in the primary UDM melt (third constraint).

Solving mass balance equations (1) and (2) for the above constraints and using reasonable values of φ (0.60–0.65), F_E (0.5), F_{PE} (0.10–0.15), F_{PX} (0.45), X_{PX} (0.60), $K_{PX}^{Sr} = 0.05$, $K_{PE}^{Sr} = 0.01$ and $K_E^{Sr} = 0.15$ (see the discussion on these parameters in ref. 27) gives a relation between contents and isotope composition of Sr in the peridotite component (Supplementary Fig. 9). Assuming a lower limit for the $^{87}Sr/^{86}Sr$ ratio of peridotite of 0.7021 (extreme depletion) yields a maximum Sr content of peridotite of about 3 p.p.m., which fulfils the conditions stated above. Thus, as expected, the peridotite source should be more depleted in Sr than average depleted MORB mantle with a Sr content of 7.66 p.p.m.[34]. For a lower content or more radiogenic Sr in peridotite, the $^{87}Sr/^{86}Sr$ in the recycled crust would be lower than 0.7090. It approaches 0.7075 (minimum allowed by the observed UDM composition) when there is no Sr in peridotite or the ratio $^{87}Sr/^{86}Sr$ in peridotite is 0.7075.

The above model is somewhat oversimplified because it uses a batch melting process and considers fixed melting phase proportions in the form of constant bulk distribution coefficients. To take into account a more realistic, aggregated critical melting process and include changing phase proportions, we further use the conceptually similar but more advanced model with melting reactions and distribution coefficients explained in ref. 27. Using the above estimates for maximum Sr content in peridotite we chose for our quantitative modelling the composition of depleted abyssal harzburgite from the database[35] with a Sr content of 2.73 p.p.m. (model 1), and a restite after 2% of near fractional melting of depleted MORB mantle[34] with a Sr content of 1.96 p.p.m. (model 2). The results of modelling are shown in Supplementary Fig. 10 and Supplementary Table 4.

The composition of recycled crust was calculated to match the trace-element composition and minimum $^{87}Sr/^{86}Sr = 0.7075$ ratio of UDM primary melt. For $^{87}Sr/^{86}Sr = 0.7021$ of peridotite, the results for recycled crust are $^{87}Sr/^{86}Sr = 0.7086$

(model 1) and 0.7083 (model 2). The estimated trace-element compositions of recycled crust correspond to highly depleted oceanic crust and are reasonably close to reported compositions of depleted MORBs[36,37] (Supplementary Fig. 10a). The compositions of peridotites correspond to depleted abyssal harzburgite or depleted lherzolite (Supplementary Fig. 10a). We conclude that the highly radiogenic Sr and the chemical composition of Mauna Loa ultra-depleted melts can be produced by recycling, melting and reacting of depleted oceanic crust altered by sea water and depleted mantle peridotite. This peridotite may be also a part of the recycled oceanic lithosphere.

We further investigate an alternative possibility for the production of highly radiogenic Sr in ultra-depleted melt by the involvement of small amounts of continental sediments with an extremely high $^{87}Sr/^{86}Sr$ ratio. We use the same model as model 1 but for $^{87}Sr/^{86}Sr = 0.7025$ of recycled oceanic crust and variable amounts of sediment with the most extreme $^{87}Sr/^{86}Sr = 0.7349$ (from Sumatra[38]). This yields an amount of 1.6% of such sediment in the recycled component to match $^{87}Sr/^{86}Sr = 0.7075$ of the final melt. However, this substantially increases the concentration of highly incompatible elements such as Th and La of the final melt and significantly lowers its Nb/Th ratio (Supplementary Fig. 10d and Supplementary Table 4). We conclude that recycled continental material, even with extremely radiogenic Sr, cannot produce the highly incompatible trace-element pattern of Mauna Loa UDMs.

32. Jarosevich, E. J., Nelen, J. A. & Norberg, J. A. Reference sample for electron microprobe analysis. *Geostand. Newsl.* **4,** 43–47 (1980).
33. Jochum, K. P. *et al.* The preparation and preliminary characterization of eight geological MPI-DING reference glasses for in-situ microanalysis. *Geostand. Newsl.* **24,** 87–133 (2000).
34. Workman, R. K. & Hart, S. R. Major and trace element composition of the depleted MORB mantle (DMM). *Earth Planet. Sci. Lett.* **231,** 53–72 (2005).
35. Niu, Y. L. Bulk-rock major and trace element compositions of abyssal peridotites: implications for mantle melting, melt extraction and post-melting processes beneath mid-ocean ridges. *J. Petrol.* **45,** 2423–2458 (2004).
36. Saal, A. E., Hauri, E. H., Langmuir, C. H. & Perfit, M. R. Vapour undersaturation in primitive mid-ocean-ridge basalt and the volatile content of Earth's upper mantle. *Nature* **419,** 451–455 (2002).
37. Bach, W., Peucker-Ehrenbrink, B., Hart, S. R. & Blusztajn, J. S. Geochemistry of hydrothermally altered oceanic crust: DSDP/ODP Hole 504B—implications for seawater–crust exchange budgets and Sr- and Pb-isotopic evolution of the mantle. *Geochem. Geophys. Geosyst.* **4,** doi:10.1029/2002GC000419 (2003).
38. Plank, T. & Langmuir, C. H. The chemical composition of subducting sediment and its consequences for the crust and mantle. *Chem. Geol.* **145,** 325–394 (1998).

doi:10.1038/nature10321

Samples and data

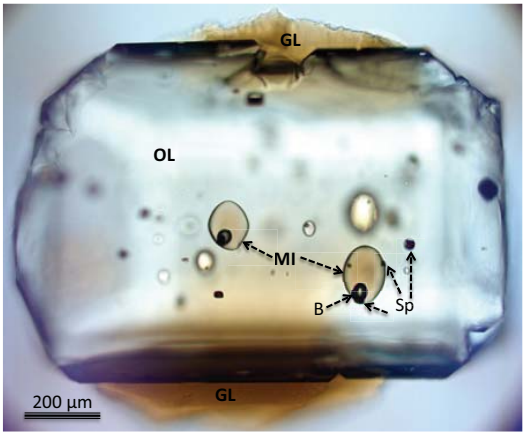

Fig. S1. Puu Wahi, Mauna Loa, Hawaii euhedral olivine (OL) with melt inclusions (MI) and surrounded glass (GL). Melt inclusions consist of fresh glass and contain spherical shrinkage bubbles (B), chromium spinel crystals (Sp) and occasionally small droplets of sulfide melt.

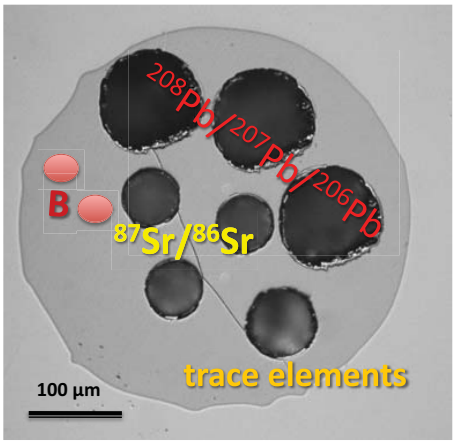

Fig. S2. Reflected light image of melt inclusion in olivine exposed on the surface illustrating all applied in-situ analytical techniques. Three large (100 µm) laser pits are for Pb isotopes, three (50 µm) for Sr isotopes, and one (60 µm) for trace elements. The position of two ion probe pits (ca 20 µm) for B analysis is indicated by red ovals. Three electron probe spots of 3 µm for analysis of major elements and Cl and S are almost invisible in the center of inclusion.

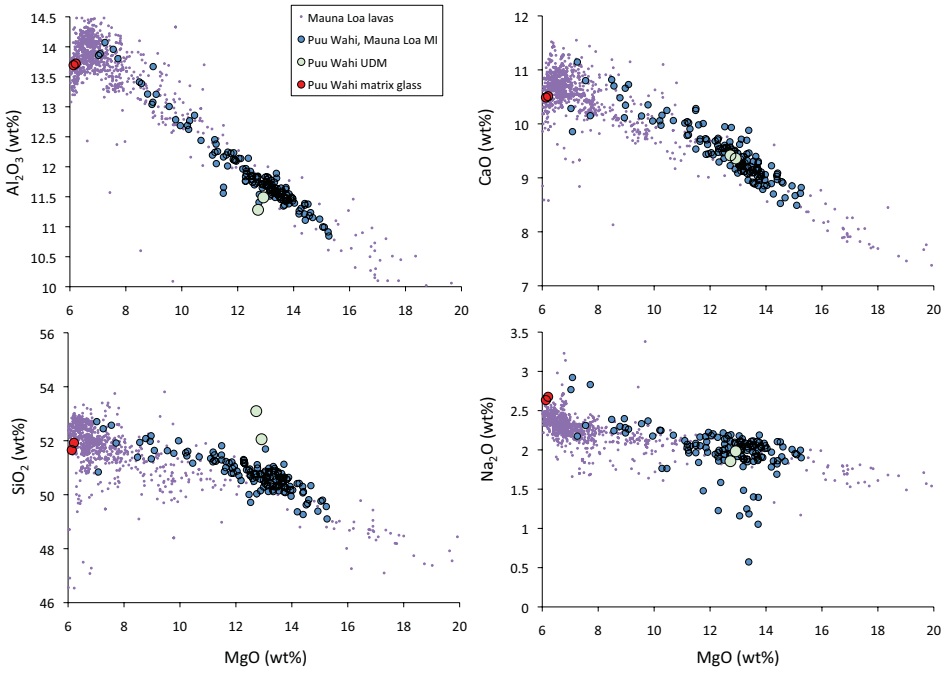

Fig. S3. Composition of melt trapped in olivine phenocrysts recalculated to equilibrium with host olivine (see ref 27 for calculation details).
Note that UDMs are similar to typical Mauna Loa melt inclusions and lavas in concentrations of Ca, Na, but are slightly enriched in Si and depleted in Al.

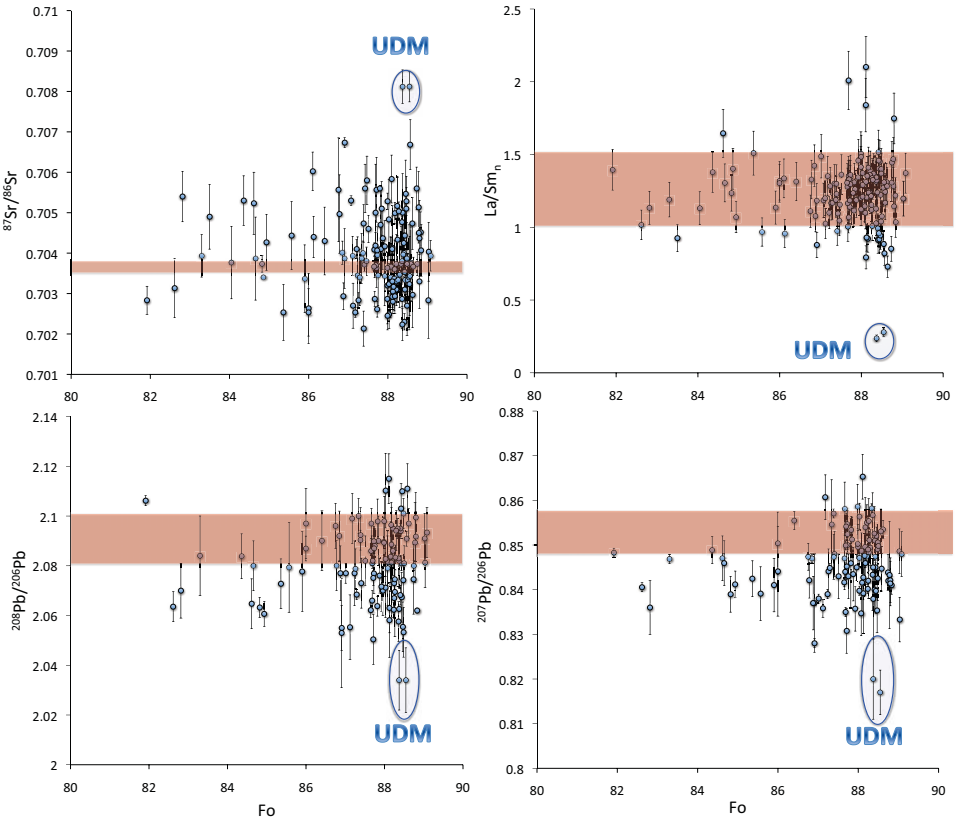

Fig. S4. Relation between compositions of Puu Wahi, Mauna Loa, melt inclusions and host olivine. Red field illustrates range of compositions of recent Mauna Loa lavas according to GEOROC database. Error bars: one standard error. Outlined are ultra-depleted melt inclusions (UDM).

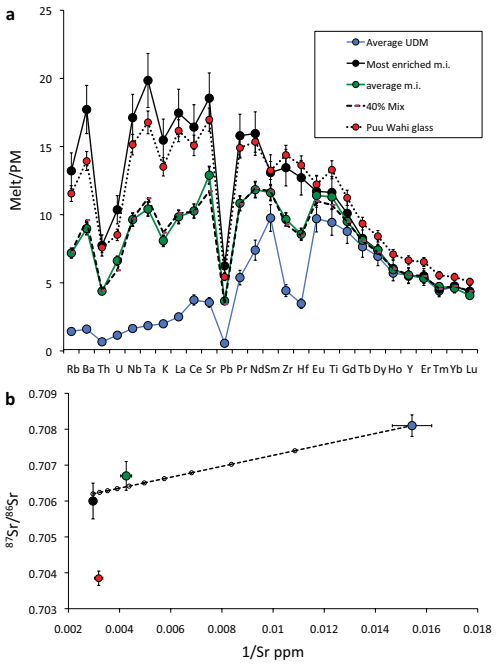

Fig. S5. Mixing behavior of melts with 87Sr/86Sr > 0.7060.

a. Primitive-mantle normalized concentrations of incompatible elements. Average UDM: average of two UDM melt inclusions (m.i.) (116 and 109); Most enriched m.i.: Most enriched melt inclusion in the suite (1112b); Average m.i.: average of two intermediate melt inclusions (118 and 1229); 40% Mix: mixture of Ave UDM and Most enriched m.i. in the proportions of 40:60.

b. 1/Sr concentration versus 87Sr/86Sr on a mixing line between the most enriched and the most depleted melt inclusions. Ave UDM is the pooled average of 21 measurements of two UDM melt inclusions (116 and 109, see methods); Most enriched m.i. is the pooled average of 4 measurements of inclusion 1112b; Ave m.i. is the pooled average of 9 analyses of melt inclusions 118 and 1229. Dashed line represents mixture of the most depleted and most enriched inclusion, the latter with 87Sr/86Sr ratio of 0.7062 slightly higher than the mean ratio 0.7060, but within 1 standard error of the mean. Small solid circles indicate 10% increments of the mixing proportions. Error bars: one standard error.

Note that mixing proportions of end-members in intermediate melt inclusions are almost identical (at 40% UDM component) for all trace elements and Sr isotopes. Also note that the binary mixing relationship illustrated here explains part of the compositional array of the melt inclusions quite well, but the Puu Wahi bulk glass composition does not lie on this mixing array.

Isotope data quality

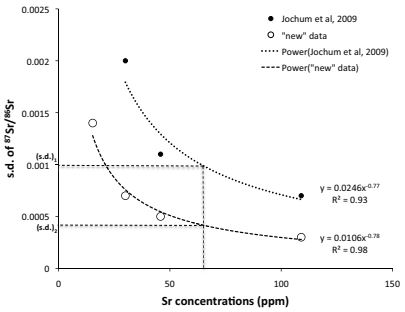

Figure S6. Standard deviation (s.d.) versus Sr concentration in low Sr reference glasses. Thin dashed lines represent predicted external one standard error for individual measurements of UDMs with Sr concentration level of 65 μg/g: $(s.d)_1$= 0.0010- for "old" data set[29], $(s.d.)_2$=0.0004 - for "new" data set.

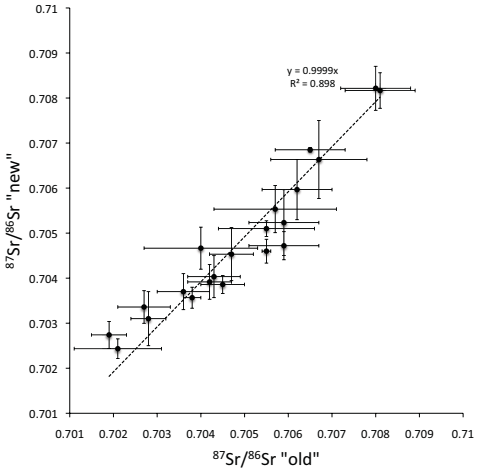

Figure S7. 21 reanalyzed melt inclusions shown with one standard error of mean. "New" data match "old" one very well, being significantly more precise.

The mineralogy of Hawaiian source

The excess of Ni in Hawaiian olivines compared to olivine in equilibrium with peridotite-derived melt has been explained by contribution of a melt derived from olivine-free pyroxenite[27]. This explanation relies on the assumption that the partition coefficient of Ni between olivine and melt depends only on the composition of melt and olivine[39]. Recent papers[40,41] have suggested new models for Ni partitioning between olivine and melt, which consider temperature dependences in addition to compositional dependence. These models imply that high nickel content of Hawaiian olivines might simply be due to adiabatic cooling of melts initially generated at high temperature and pressure. It is well known that temperature and compositional effects are strongly interrelated and are therefore very difficult to separate experimentally. We have already discussed this possibility and have noted[27]: *"It is conceivable that there is a temperature effect in addition to, but difficult to separate from, the compositional effect on Ni partitioning. In that case, the high nickel content of Hawaiian olivines might simply be due to adiabatic cooling of melts initially generated at high temperature and pressure. If that were true, one would expect a similar effect for all equally high pressure–temperature melts such as Gorgona komatiites or west Greenland picrites. However, Gorgona and west Greenland olivines show that this effect, if present at all, is too small to explain the Ni excess in Hawaiian olivines (Fig. 1)."*

This issue clearly demonstrated by figure S8 showing significant Ni excess in Puu Wahi, Mauna Loa olivine (including UDM hosted olivine grains) compare to olivine from Munro Township komatiite and olivine equilibrium with peridotite-derived melt. Composition of olivine from komatiite is reasonably consistent with crystallization of peridotite-derived melt with high MgO content (24-30 wt.%). The olivine from Puu Wahi, Mauna Loa has on average about 35% excess of Ni over olivine with the same Fo content, which should crystallize from peridotite-derived melt with initial MgO=20wt%. This amount of MgO is the maximum estimate for the primary Hawaiian melts[27,41,42]. Because komatiite primary melt has been derived at higher pressures and temperatures than Mauna Loa primary melt[27,43] additional to composition temperature affect on Ni partition between olivine and melt must, if present, cause higher Ni contents of low pressure komatitic olivines. This is clearly not the case.

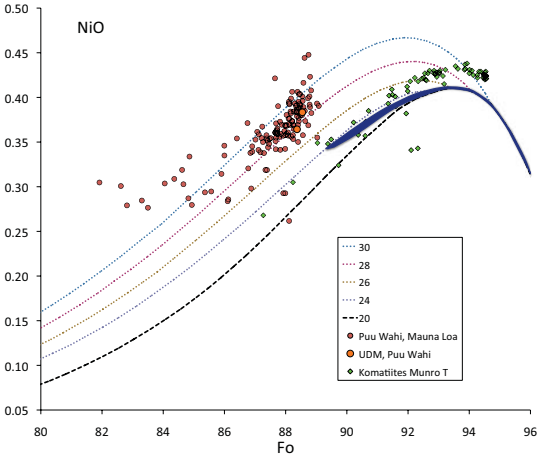

Figure S8. Comparison of composition of Puu Wahi, Mauna Loa olivine with olivine from peridotite-derived melt, represented by olivines from Munro Township komatiite (sample M-666), ref. 28. Errors for data are within symbol sizes. The dotted lines represent compositions of olivine crystallized at 1 bar pressure from peridotite-derived melts with different initial MgO contents (20, 24, 26, 28, 30 % MgO)[42]. Blue field indicates compositions of olivine in equilibrium with primary peridotite-derived melts with 8-38 wt.% MgO (ref. 42). Anomalously low Ni contents of a few olivine grains in both Mauna Loa and komatiite samples may indicate interaction with sulfide melt.

In addition, it is shown by C. Herzberg, 2011(ref. 42) and C. Herzberg, 2011 (personal communication) that models of C. Li et al, 2010 (ref. 40) and K. Putirka et al., 2011 (ref. 41) for Ni partitioning between olivine and melt reproduce experimental data much less accurate than Beattie et al, 1991 model[39]. In particular, these models underestimate distribution coefficients of Ni between olivine and melt for the high temperature and pressure which results in overestimation of Ni content of olivine crystallized from adiabatically decompressed melt at the surface[42]. We thus conclude that the composition of Mauna Loa olivine could not be explained by unconsidered temperature effect on olivine-melt Ni partition and argues for the significant role of non-peridotitic (pyroxenitic) lithology in their mantle source.

Modeling

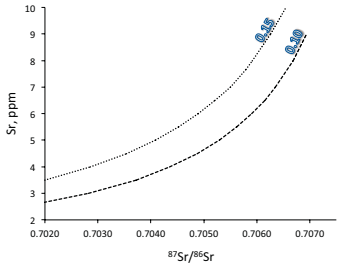

Figure S9. Maximum amount of Sr in peridotite component as a function of its isotope composition. Numbered lines are solutions of equations 1,2 for degree of batch melting of peridotite F_{PE}= 0.15 and 0.10 respectively (fraction of 1).

Figure S9 shows that peridotite component in the source of UDM should have maximum content of Sr of around 3 ppm if its $^{87}Sr/^{86}Sr$ ratio is 0.7021 (extreme depletion). Using this constraint we chose for a quantitative modeling the composition of depleted abyssal harzburgite from the database of Y. Niu, 2004, ref. 35 (sample IO11-76-59-24 from Islas Ocades, South West Indian Ridge) with Sr content of 2.73 ppm (*model 1*), and a calculated restite after 2% of near fractional melting of DMM with a Sr content of 1.96 ppm (*model 2*). The results of modeling are shown in Supplementary information (see Fig S10 and table S4). We use three stages model with melting reactions and distribution coefficients explained in ref. 27 and crystal-melt partition coefficients and melting reactions from ref. 13.

First stage: formation of pyroxenite by reaction of aggregated partial melt of eclogite (F_E =0.5) with peridotite in proportions 0.67:0.33, matching amount of olivine in this harzburgite.

Second stage: critical partial melting of pyroxenite (F_{PX} =0.45) and peridotite (F_{PE} =0.15).

Third stage: mixing of pyroxenite-derived melt and peridotite derived melt in proportions 0.60:0.40 (X_{PX}=0.60). These conditions correspond to overall fraction of recycled crust in the peridotite of 21% and agree with earlier estimations for Mauna Loa lavas[27]. We refer this model setup as *model 1*. We also used same model with two other input conditions:

model 2. Conditions the same as model 1, but with depleted lherzolite produced by 2% wt. near fractional melting (0.05wt% residual porosity) of average DMM composition[34]. Because peridotite in this model contains 60%wt olivine, we used following proportions of aggregated partial melt of eclogite and peridotite 0.60:0.40 in the pyroxenite forming reaction.

model 3. Conditions the same as model 1, but the recycled crust contains 1.6% of continental sediments with extremely radiogenic Sr: Sumatra sediments, 87Sr/86Sr=0.7349, ref[38].

For comparison with the calculated ocean crust compositions *model 1E* and *model 2E*, we show composition of a highly depleted MORB sample A25-D20-5 from the Siqueiros Fracture zone[36] and from dyke, site 504B (sample 504B.193.R1.58-60), ref. 37.

39. Beattie, P., Ford, C. & Russell, D. Partition-Coefficients for Olivine-Melt and Ortho-Pyroxene-Melt Systems. *Contributions to Mineralogy and Petrology* **109**, 212-224 (1991).
40. Li, C. S. & Ripley, E. M. The relative effects of composition and temperature on olivine-liquid Ni partitioning: Statistical deconvolution and implications for petrologic modeling. *Chemical Geology* **275**, 99-104, doi:10.1016/j.chemgeo.2010.05.001 (2010).
41. Putirka, K., Ryerson, F. J., Perfit, M. & Ridley, W. I. Mineralogy and Composition of the Oceanic Mantle. *Journal of Petrology* **52**, 279-313, doi:10.1093/petrology/egq080 (2011).
42. Herzberg, C. Identification of Source Lithology in the Hawaiian and Canary Islands: Implications for Origins. *Journal of Petrology* **52**, 113-146, doi:10.1093/petrology/egq075 (2011).
43. Arndt, N. Komatiites, kimberlites, and boninites. *Journal of Geophysical Research-Solid Earth* **108** (2003).
44. Hofmann, A. W. Chemical differentiation of the Earth: the relationship between mantle, continental crust, and oceanic crust. *Earth Planet. Sci. Lett.* **90**, 297-314 (1988).

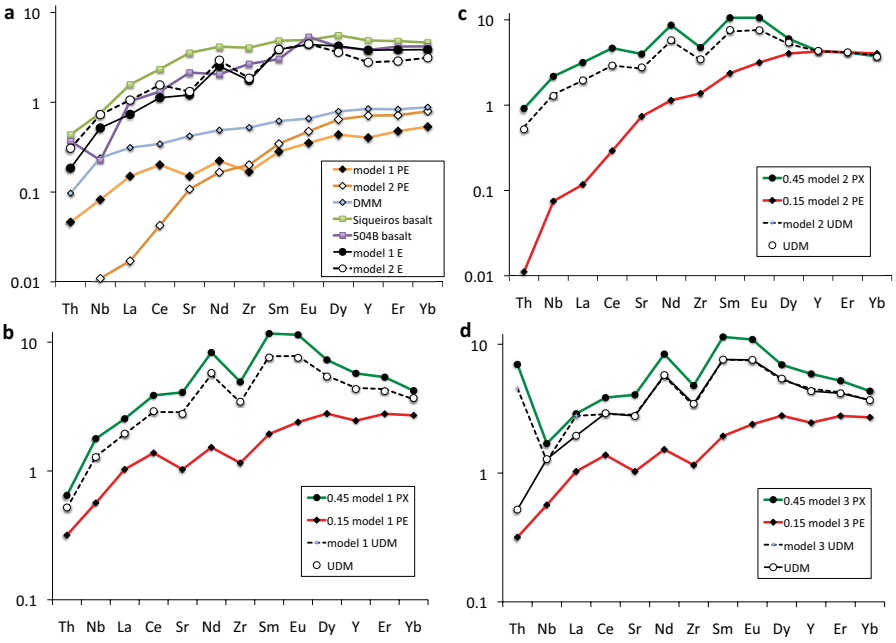

Figure S10. Results of modeling. a. Compositions of recycled oceanic crust (E) and peridotite (PE) for *models 1,2*. Siqueiros basalt and 504B basalt stand for compositions of depleted oceanic crust[36,37], DMM-average depleted mantle[34]. **b.** Composition peridotite-derived melt (PE), pyroxenite-derived melt (PX) and result of their mixing (*model 1* UDM) for *model 1* compared with composition of UDM primary melt (UDM). **c.** Same as b but for *model 2*. **d.** Same as (b) but for *model 3*. All compositions are normalized to primitive mantle composition[44].